LETTERS

A stepwise mechanism for acetylcholine receptor channel gating

Prasad Purohit[1], Ananya Mitra[1] & Anthony Auerbach[1]

Muscle contraction is triggered by the opening of acetylcholine receptors at the vertebrate nerve–muscle synapse[1–4]. The M2 helix of this allosteric membrane protein lines the channel, and contains a 'gate' that regulates the flow of ions through the pore. We used single-molecule kinetic analysis to probe the transition state of the gating conformational change and estimate the relative timing of M2 motions in the α-subunit of the murine acetylcholine receptor[5]. This analysis produces a 'Φ-value' for a given residue that reflects its open-like versus closed-like character at the transition state. Here we show that most of the residues throughout the length of M2 have a Φ-value of ~0.64 but that some near the middle have lower Φ-values of 0.52 or 0.31, suggesting that αM2 moves in three discrete steps. The core of the channel serves both as a gate that regulates ion flow and as a hub that directs the propagation of the gating isomerization through the membrane domain of the acetylcholine receptor.

Nicotinic acetylcholine receptors (AChRs) are ion channels that gate between ion-impermeable closed (C) and ion-permeable open (O) conformations. The membrane domain of each of the five AChR subunits has four helices (M1–M4). The structure of the unliganded-closed *Torpedo* AChR (at 4 Å resolution) shows that a narrow part of the channel is formed by residues at the mid-section of the second transmembrane helix, M2[6,7]. Here, interactions between side chains in different subunits form a 'hydrophobic girdle' that presumably shuts off ion flow in the C conformation and, hence, might act as a gate[6]. Results obtained with substituted cysteine[8,9] or histidine[10] accessibility methods suggest that the main barrier to the diffusion of ions in closed AChRs is near the cytoplasmic limit of M2. However, similar experiments with other Cys-loop receptors indicate that in these closely-related proteins it is the middle of M2 that serves this function[11,12]. Computational studies[13] support the idea that the middle of M2 is a barrier to ionic conduction, and mutagenesis[14] and accessibility[15] studies show that M2 equatorial residues move during C↔O gating, as required for a gate.

The αM2 helix comprises 27 residues that run from the intracellular limit of the membrane (1′) to the extracellular domain (27′; Fig. 1). The character of the di-liganded, C↔O transition state ensemble (TSE) was probed by measuring the single-channel opening (k_o) and closing (k_c) rate constants for sets of side chain substitutions of individual amino acids. The intermediates of the gating reaction are too brief to be observed directly but some properties of the TSE can be deduced from Φ, the slope of a log–log plot of k_o versus K_{eq} (k_o/k_c) for each mutational series[16]. One interpretation of Φ is that it gives the relative timing of the movement of the perturbed residue, with higher values indicating earlier, and similar values indicating temporally-correlated, gating motions[5] (see Methods).

Φ-values have been reported previously for three αM2 residues, S27′ (0.64), V17′ (0.61) and L9′ (0.26)[17]. The step decrease in Φ in αM2 (0.35 units between 17′ and 9′) is roughly similar in magnitude and location to that in δM2 (0.25 units between 12′ and 9′)[18]. We interpret these breakpoints in Φ to indicate that in the α- and δ-subunits the upper part of M2 moves before the middle. That is, in both subunits the mid-section of M2 appears to be a flexible junction.

We focused our attention on the αM2 residues between 16′ and 2′, a region that forms a narrow bore of the channel and brackets the presumptive gate[6]. Figure 2 shows Φ-value analyses for 12 αM2 positions (Supplementary Fig. 1 and Supplementary Tables 1 and 2). Mutations of three additional positions (S10′, I5′ and T2′) exhibited only wild-type gating kinetics. This result makes it unlikely that these residues, one of which sets the conductance of the open channel (2′)[19], are moving parts of a 'gate', but does not rule out gating motions below 2′[9,10,20]. We cannot conclude definitively that a small excursion in K_{eq} indicates that there is relatively less gating motion (for example, at the cytoplasmic end of M2), because little or no change may be apparent if a side chain and its local environment move in register, and because the magnitude of the change in K_{eq} may not reflect the magnitude of a residue's motion.

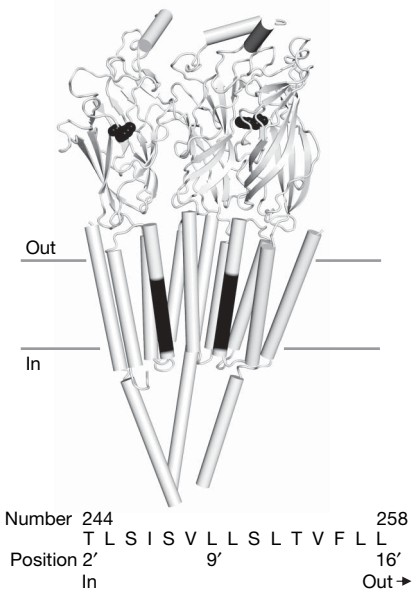

Figure 1 | The location of αM2. The α_δ-, ε- and α_ε-subunits of the AChR; for clarity the δ- and β-subunits are not shown. The thick horizontal lines mark the approximate location of the membrane. The M2 helix forms the lumen of the channel. In each α-subunit, in black is residue W149 at the two transmitter binding sites and residues 17′–2′ (top to bottom) in each αM2 helix. The distance from W149 to the 9′ residue of αM2 is ~60 Å (*Torpedo* AChR, PDB database accession number 2bg9.pdb). Below, the amino acid sequence (N-to-C) of M2 in the mouse α-subunit. K0′ and E−1′ are likely to be in the cytoplasmic domain and E20′ is likely to be the first residue in the extracellular ionic compartment.

[1]Department of Physiology and Biophysics, State University of New York at Buffalo, Buffalo, New York 14214, USA.

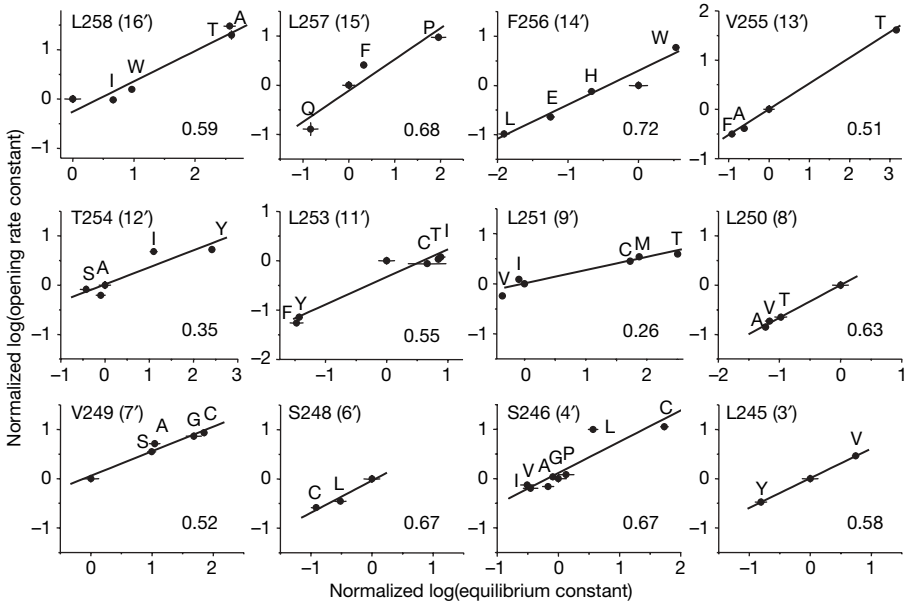

Figure 2 | Φ-value analysis. Plots of normalized log opening rate constant (k_o) against normalized log equilibrium constant ($K_{eq} = k_o/k_c$, where k_c is the closing rate constant) for 12 positions between 16′ and 3′. The wild-type (WT) side chain ($K_{eq} = 0$) is unlabelled; both the rate and equilibrium constants were normalized by the WT values. Three additional αM2 positions are not shown because all constructs exhibited only WT gating kinetics (S10′→A, T, V; I5′→A, G, S, T, W; and T2′→A, C, I). The plots for αM2 positions 27′, 17′ and 9′ were reported previously[17]. The error bars (for both k_o and K_{eq}) are ± s.e.m. (Supplementary Table 1). Φ, the slope of the plot (estimated using the inverse errors on both axes as weights), is shown at lower right of each plot (Supplementary Table 2).

Of the 13 positions between 17′ and 2′ that were sensitive to mutation, six (17′, 16′, 15′, 12′, 9′ and 7′) mainly increased and three (14′, 8′ and 6′) mainly decreased K_{eq}. At four positions (13′, 11′, 4′ and 3′) side-chain substitutions either increased or decreased K_{eq}, by up to ~100-fold. The mutated residues are far from the transmitter binding sites (Fig. 1), and we hypothesize that these changes in K_{eq} arise mainly from parallel changes in the unliganded gating equilibrium constant rather than from changes in the closed/open affinity ratio[21] (Supplementary Fig. 2).

Nine αM2 residues had Φ-values between 0.59 and 0.72 (Fig. 3 and Supplementary Table 2). Included in this group are residues near the cytoplasmic limit (3′), close to the equator (8′), in the upper half (17′) and at the extracellular limit of the helix (27′). We conclude that during di-liganded gating, the movements of most of αM2, from amino to carboxy terminus, are correlated temporally, with $\Phi \approx 0.64$.

Two clearly exceptional residues were 9′ ($\Phi = 0.26$) and 12′ ($\Phi = 0.35$), both of which are near the αM2 equator. The average Φ for these two residues (0.31) is similar to those in the lipid-facing surface of αM3 (0.30)[22], the upper half of δM2 (0.31)[18], the M2 9′ residues of the β- and ε-subunits (0.32)[17] and εM4 (0.33)[23]. Three other αM2 mid-section residues (13′, 11′ and 7′) had Φ-values of 0.51, 0.48 and 0.52, respectively. A weighted k-means cluster analysis of Φ-values for all αM2, αM3 and αM4 residues (Fig. 3a) shows that there are only three populations of Φ value in these domains; it also shows that 13′+11′+7′ and 9′+12′ are distinct from the bulk of αM2 and instead belong to the αM4 and αM3 populations, respectively. We conclude that the gating motions of αM2 probably occur in three steps, with most of the residues throughout the length of the helix moving first ($\Phi = 0.64$), followed by 13′+11′+7′ ($\Phi = 0.52$), followed by 12′+9′ ($\Phi = 0.31$).

The motions of M2 are part of the overall AChR isomerization, in which domains having temporally correlated gating motions ('Φ-blocks') move in sequence to generate a propagated, brownian conformational 'wave' (Fig. 4)[24,25]. In the α-subunit, agonist binding triggers the movement of loops A, B and C in the extracellular domain, which causes a ~10^4-fold increase in the affinity for ACh at each of the two transmitter binding sites ($\Phi \approx 0.93$; purple in

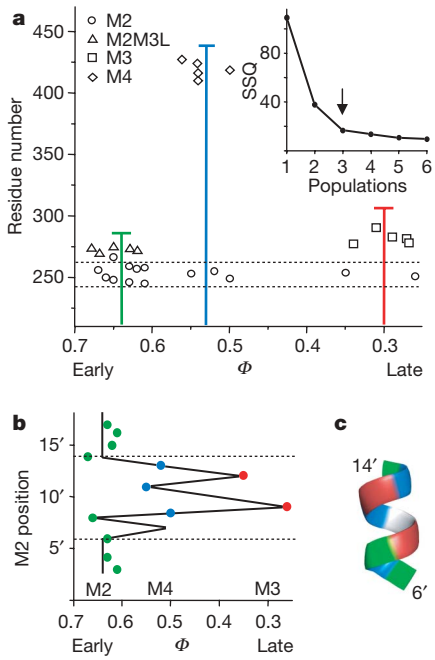

Figure 3 | Distribution of Φ-values. **a**, Statistical analysis of Φ-values for α-subunit residues in M2, the M2-M3 linker (M2M3L) (A. Jha, D. Cadugan, P.P. and A.A., manuscript in preparation), M3[22] and M4[17] (Supplementary Methods). The Φ-values are clustered into three populations (mean ± s.d.): 0.64 ± 0.02 (green), 0.52 ± 0.02 (blue) and 0.30 ± 0.03 (red). Inset, the total sum squared deviation (SSQ) shows that there are three populations of Φ. The αM2 equator has residues in all three populations. **b**, Expansion of the dashed region in **a**. Most of the residues throughout the length of αM2 move relatively early in the gating reaction, but some at the mid-section (7′–13′) move later. No Φ-values are shown for 2′, 5′ and 10′ because mutations here did not significantly change K_{eq}. The order of motion is M2 > M4 > M3. **c**, Cartoon structure (*Torpedo* AChR, PDB accession number 2bg9.pdb) of the dashed region in **b**, coloured by Φ-value (see above; white, <3-fold change in K_{eq}).

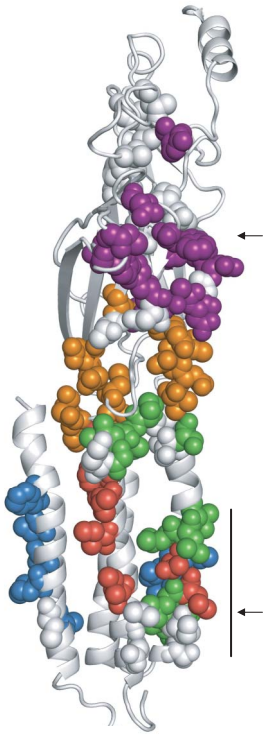

Figure 4 | Map of Φ-values. In the α-subunit shown, Φ-values are clustered spatially and decrease discontinuously between the transmitter binding site and the gate. The vertical line (~20 Å) marks the lumen of the channel, and the upper and lower arrows indicate W149 (at the transmitter binding site) and L251 (at the gate). The cytoplasmic domain (M3–M4 linker) is not shown. The residues that have been examined for Φ-value are shown as spheres[17,21,23,25,26] (A. Jha, D. Cadugan, P.P. and A.A., manuscript in preparation). The colours are according to Φ-value: purple, >0.90; orange, 0.75–0.85; green, 0.59–0.72; blue, 0.48–0.57; red, 0.26–0.35; white, no Φ value (change in K_{eq} < 3-fold). The map suggests that AChR gating is a brownian conformational cascade of domain motions that link an affinity change for agonists at the binding site with a permeability change for ions in the pore (α_ε-subunit, *Torpedo* AChR, PDB accession number 2bg9.pdb).

Fig. 4)[21,25]. This local conformational change then triggers the movement of residues at the base of the extracellular domain, in loop 7 (the Cys-loop) and loop 2 ($\Phi \approx 0.78$; orange)[26]. Next, residues in the M2-M3 linker (A. Jha, D. Cadugan, P.P. and A.A., manuscript in preparation) and throughout most of αM2 move approximately synchronously ($\Phi \approx 0.64$; green), followed in sequence by αM4 and the 13′, 11′ and 7′ residues at the αM2 mid-section ($\Phi \approx 0.52$; blue). Finally, 12′ and 9′ in αM2 move, along with residues in the above-mentioned domains of the α-, β-, δ- and ε-subunits ($\Phi \approx$ 0.30; red), at which point we speculate that ions begin to flow rapidly through the pore. Together, these reversible domain motions provide the framework, if not the structural details, of the AChR channel-opening conformational change.

Two residues have been proposed as key points of energy transfer between the extracellular domain and αM2. Unwin[7] proposed that V46 in loop 2 ($\Phi = 0.78$) interacts with S269 in M2 ($\Phi = 0.64$) to drive opening by a 'pin-into-socket' mechanism. Lummis *et al.*[27] and Lee and Sine[28] suggested that the motion of a proline in the M2-M3 linker (P272 in AChRs) is coupled to the gating motion of M2 by a *cis–trans* isomerization or through interactions with a nearby salt bridge (R209–E45) plus V46. Residues in the M2-M3 linker (including P272) have a Φ-value of ~0.64 (A. Jha, D. Cadugan, P.P. and A.A., manuscript in preparation), which indicates that this region moves synchronously with αM2, after the motion of F135 in the Cys-loop ($\Phi = 0.78$). Also, the pairs F135–P272 and V46–S269 are both at the boundary between the 0.78 and 0.64 Φ-blocks, and mutation of all four of these residues significantly changes K_{eq}.

The propagation of gating energy appears to not be concentrated at a single 'on-off' switch but rather to be spread over at least four Φ-block boundaries ($0.93 \leftrightarrow 0.78 \leftrightarrow 0.64 \leftrightarrow 0.52 \leftrightarrow 0.31$), with the exchange of energy at each boundary occurring at multiple sites. AChR gating (the conformational pathway through the TSE) is neither instantaneous nor smooth but instead is characterized by back-and-forth, brownian motion of nanometre-sized domains, on the 10–100 ns timescale[24].

The Φ-values suggest that the channel opening motions in the membrane are asynchronous. The ends of αM2 move first, then the αM2 centre-flanking regions along with αM4, then the 12′ and 9′ residues of αM2 along with the 9′ residues of βM2, εM2 and αM3. In the δM2 segment, the extracellular end moves about this time, followed by the 9′ residue and the intracellular end[18]. Although our experiments do not address directly whether or not the conformational changes at the middle of M2 regulate ionic conductance, the pattern of Φ-values support the following notion. A 'gate' is located at the middle of M2 (between 9′ and 12′); this gate's structure regulates ionic conductance by movements in the α-subunits that subsequently propagate to the other subunits, rather than by a synchronous, symmetrical motion in all subunits. Previously it was shown that in hybrid AChRs (having only one mutated α-subunit) the two 17′ positions have the same Φ-value but the 9′ positions have different Φ-values (0.0 and 0.32) and, hence, move asynchronously[17]. Because $\Phi = 0.26$ for the double 9′ mutant, we speculate that the difference in Φ for 9′ occurs only in the hybrid constructs and that the gating motions in the M2 double mutants are synchronous.

The first three Φ-blocks (0.93, 0.78 and 0.64) are structurally contiguous, and their movements link the affinity changes at the two transmitter binding sites with structural changes in the region of the gate. However, it is likely that the conductance of the pore does not increase dramatically until the 'late' movements of the equatorial 13′+11′+7′ and 12′+9′ residues of αM2. Higher-resolution C and O structures and a more extensive map of Φ-values may illuminate the chemical details and evolutionary driving forces behind this three-step, doubly locked gating mechanism.

METHODS

Detailed descriptions are in Supplementary Methods. Briefly, mouse α-, β-, δ-and ε-subunits having point mutations in both α-subunits were expressed in HEK cells, and cell-attached recordings were performed using a high agonist concentration ($V_m \approx -100$ mV; 22 °C). Interval durations from selected single-channel clusters were fitted directly to estimate opening and closing rate constants. Φ is the slope of a log–log plot of opening rate-constant versus equilibrium constant for a series of mutations of each residue.

There are three plausible, non-exclusive interpretations for the physical meaning of Φ. (1) If there are many conformational pathways connecting C and O, then Φ is a function of the probabilities of traversing each of these, and reflects structural heterogeneity of the TSE. (2) If the conformation of an individual side chain at the TSE is not just either 'closed' or 'open' but can also be somewhere in between, then Φ reflects the fractional extent of reaction at the residue level (the closed- versus open-like structure of the perturbed side chain). (3) If domains sequentially and instantaneously flip conformation and in the TSE there is a mixture (with some domains 'closed' and others 'open'), then Φ reflects the fractional extent of reaction at the domain level (the closed- versus open-like structure of the protein when the perturbed side chain flips). All of these interpretations are consistent with an apparent two-state reaction.

The AChR is large, and undoubtedly there are metastable intermediates between stable C and stable O. Experiments show that the net dynamics across the TSE are slow (~μs^{-1})[29] and that the map of Φ is organized. There are spatially contiguous groups of residues that have approximately the same Φ-value, and there is an approximately longitudinal gradient in Φ that decreases discontinuously between the transmitter binding site and the gate (Fig. 4)[23,25]. A two-pathway mechanism ($\Phi = 0$ and 1) cannot explain some fractional Φ-values[18], and only the domain-level interpretation predicts such an organized Φ map. We hypothesize that Φ reflects the fractional extent of reaction at the domain level and, hence, gives the relative timing of the perturbed residue's motion within the overall reaction cascade[24].

Received 20 December 2006; accepted 28 February 2007.

1. Edelstein, S. & Changeux, J.-P. Allosteric transitions of the acetylcholine receptor. *Adv. Protein Chem.* **51,** 121–184 (1998).
2. Karlin, A. Emerging structure of the nicotinic acetylcholine receptors. *Nature Rev. Neurosci.* **3,** 102–114 (2002).
3. Lester, H. A., Dibas, M. I., Dahan, D. S., Leite, J. F. & Dougherty, D. A. Cys-loop receptors: New twists and turns. *Trends Neurosci.* **27,** 329–336 (2004).
4. Sine, S. M. & Engel, A. G. Recent advances in Cys-loop receptor structure and function. *Nature* **440,** 448–455 (2006).
5. Zhou, Y., Pearson, J. E. & Auerbach, A. Φ-Value analysis of a linear, sequential reaction mechanism: Theory and application to ion channel gating. *Biophys. J.* **89,** 3680–3685 (2005).
6. Miyazawa, A., Fujiyoshi, Y. & Unwin, N. Structure and gating mechanism of the acetylcholine receptor pore. *Nature* **423,** 949–955 (2003).
7. Unwin, N. Refined structure of the nicotinic acetylcholine receptor at 4 Å resolution. *J. Mol. Biol.* **346,** 967–989 (2005).
8. Akabas, M. H., Kaufmann, C., Archdeacon, P. & Karlin, A. Identification of acetylcholine receptor channel-lining residues in the entire M2 segment of the α-subunit. *Neuron* **13,** 919–927 (1994).
9. Wilson, G. G. & Karlin, A. The location of the gate in the acetylcholine receptor channel. *Neuron* **20,** 1269–1281 (1998).
10. Paas, Y. *et al.* Pore conformations and gating mechanism of a Cys-loop receptor. *Proc. Natl Acad. Sci. USA* **102,** 15877–15882 (2005).
11. Bali, M. & Akabas, H. The location of closed channel gate in Cys-loop receptor channels. *J. Gen. Physiol.* (in the press).
12. Panicker, S., Cruz, H., Arrabit, C. & Slesinger, P. A. Evidence for a centrally located gate in the pore of a serotonin-gated ion channel. *J. Neurosci.* **22,** 1629–1639 (2002).
13. Beckstein, O. & Sansom, M. S. P. A hydrophobic gate in an ion channel: The closed state of the nicotinic acetylcholine receptor. *Phys. Biol.* **3,** 147–159 (2006).
14. Labarca, C. *et al.* Channel gating governed symmetrically by conserved leucine residues in the M2 domain of nicotinic receptors. *Nature* **376,** 514–516 (1995).
15. Pascual, J. M. & Karlin, A. State-dependent accessibility and electrostatic potential in the channel of the acetylcholine receptor. inferences from rates of reaction of thiosulfonates with substituted cysteines in the M2 segment of the α subunit. *J. Gen. Physiol.* **111,** 717–739 (1998).
16. Leffler, J. E. & Grunwald, E. *Rates and Equilibria of Organic Reactions as Treated by Statistical, Thermodynamic, and Extrathermodynamic Methods* (Wiley, New York, 1963).
17. Mitra, A., Cymes, G. D. & Auerbach, A. Dynamics of the acetylcholine receptor pore at the gating transition state. *Proc. Natl Acad. Sci. USA* **102,** 15069–15074 (2005).
18. Cymes, G. D., Grosman, C. & Auerbach, A. Structure of the transition state of gating in the acetylcholinereceptor channel pore: A Φ-value analysis. *Biochemistry* **41,** 5548–5555 (2002).
19. Villarroel, A., Herlitze, S., Koenen, M. & Sakmann, B. Location of a threonine residue in the α-subunit M2 transmembrane segment that determines the ion flow through the acetylcholine receptor channel. *Proc. R. Soc. Lond. B* **243,** 69–74 (1991).
20. Zhang, H. & Karlin, A. Contribution of the beta subunit M2 segment to the ion-conducting pathway of the acetylcholine receptor. *Biochemistry* **37,** 7952–7964 (1998).
21. Chakrapani, S., Bailey, T. D. & Auerbach, A. The role of loop 5 in acetylcholine receptor channel gating. *J. Gen. Physiol.* **122,** 521–539 (2003).
22. Cadugan, D. J. & Auerbach, A. Conformational dynamics of the αM3 transmembrane helix during acetylcholine receptor channel gating. *Biophys. J.* (in the press).
23. Mitra, A., Bailey, T. D. & Auerbach, A. L. Structural dynamics of the M4 transmembrane segment during acetylcholine receptor gating. *Structure* **12,** 1909–1918 (2004).
24. Auerbach, A. Gating of acetylcholine receptor channels: Brownian motion across a broad transition state. *Proc. Natl Acad. Sci. USA* **102,** 1408–1412 (2005).
25. Grosman, C., Zhou, M. & Auerbach, A. Mapping the conformational wave of acetylcholine receptor channel gating. *Nature* **403,** 773–776 (2000).
26. Chakrapani, S., Bailey, T. D. & Auerbach, A. Gating dynamics of the acetylcholine receptor extracellular domain. *J. Gen. Physiol.* **123,** 341–356 (2004).
27. Lummis, S. C. R. *et al.* Cis-trans isomerization at a proline opens the pore of a neurotransmitter-gated ion channel. *Nature* **438,** 248–252 (2005).
28. Lee, W. Y. & Sine, S. M. Principal pathway coupling agonist binding to channel gating in nicotinic receptors. *Nature* **438,** 243–247 (2005).
29. Chakrapani, S. & Auerbach, A. A speed limit for conformational change of an allosteric membrane protein. *Proc. Natl Acad. Sci. USA* **102,** 87–92 (2005).

Supplementary Information is linked to the online version of the paper at www.nature.com/nature.

Acknowledgements We thank C. Grosman, P. Gottlieb and F. Sachs for discussions, and C. Nicolai, B. Steidl, M. Merritt and M. Teeling for technical assistance. This work was supported by the NIH.

Author Contributions All of the experiments and data analyses shown in Fig. 2 were performed by P.P. except for those for positions 4′ and 9′, which were performed by A.M.

Author Information Reprints and permissions information is available at www.nature.com/reprints. The authors declare no competing financial interests. Correspondence and requests for materials should be addressed to A.A. (auerbach@buffalo.edu).